A Pseudo-Potential Based Lattice Boltzmann Model to Investigate Droplet Impact onto a Thin Liquid Film

Soroush Fallah Kharmiani, Mohammad Passandideh-Fard*, and Hamid Niazmand

Department of Mechanical Engineering, Ferdowsi University of Mashhad
Mashhad, Iran

Emails: *fallah.sorou.mech.eng@gmail.com* and *mpfard@um.ac.ir*

ABSTRACT

In this paper, the pseudo-potential based lattice Boltzmann model of Li and Luo [1] is implemented to study the effect of the kinematic viscosity ratio of gas to liquid and the density ratio of liquid to gas on a droplet impact onto a thin liquid film. The model has certain capabilities which make it applicable to cases with large density ratios, low viscosities, and tunable values of surface tension independent of the density ratio. The coexistence values (densities) from the numerical model are compared to those of the analytical solution of the Maxwell construction. For further validation of the model, the simulation results for pressure difference at the interface are compared to those of the theoretical solution based on the Laplace law. Simulation results of the droplet impact onto a thin liquid film show that at high density ratios such as 1000 selected in this paper, when the kinematic viscosity ratio of the gas to liquid is high (above 150), no secondary droplets are generated. As the gas viscosity is decreased, however, the splashing leads to liquid breakup and separation of the secondary droplets. It was also found that the density ratio has a significant effect on the impact phenomenon. For a case with a low density ratio of 10, the liquid rise from the surface cannot move freely in radial and vertical directions leading to the formation of an inward liquid turn on top of the raised liquid sheet.

Key words: multiphase, pseudo-potential, lattice Boltzmann method, droplet impact

1. INTRODUCTION

Droplet impact onto a liquid film is a fascinating and complex physical phenomenon which is mostly seen in nature such as when the rain drops impinge on already wetted surfaces of the ground and ponds. It also has practical importance in industrial processes and natural sciences including fuel injection in internal combustion engines, corrosion of turbine blades, spray cooling, spray painting or coating and the erosion of soil [2,3]. Many researchers, therefore, tried to examine this subject through performing different experiments, simulations and theoretical analyses to identify the underlying physics of the phenomenon. The available results in the literature show that droplet impact onto a liquid film is governed by a set of non-dimensional numbers that among them the Weber number (ratio of the inertia to the surface tension force), the Ohnesorge number (the ratio of the viscous to surface tension force), and the dimensionless liquid film thickness (film thickness divided by the droplet diameter) are the most important ones. Furthermore, the dynamics of the impact is expressed by introducing a non-dimensional time by means of the impact velocity and the droplet diameter [3,4]. Depending on the mentioned non-dimensional parameters, different outcomes such as deposition and splashing are possible [5, 6].

Rein [5] thoroughly reviewed the experimental studies on the droplet impact onto the solid and liquid surfaces. For the impact on deep liquid layers, possible outcomes including bouncing, coalescence, vortex rings and splashing were described and the effect of different parameters, especially Weber number, on the outcome was also discussed.

Yarin and Weiss [7] experimentally and theoretically investigated the sequential impact of several droplets onto a solid surface. Generation of capillary waves in the case of low impact velocity, and liquid splashing at higher velocities were observed in their experiments. They also developed theoretical relations including the time evolution of the crown radius and compared the analytical results with the corresponding experimental data from their experiments.

Wang and Chen [8] investigated the droplet impact onto very thin liquid films and reported the critical

* corresponding author; Email: mpfard@um.ac.ir

Weber number for splashing. They found that the critical Weber number is independent of the film thickness for a dimensionless film thickness of less than 0.1; the critical Weber number, however, increases as the fluid viscosity is increased.

Manzello and Yang [9] performed experiments on water droplets impinging on water and HFE7100 (Methoxy-nonafluorobutane**)** liquid films. For their range of experiments, they observed that for the impact on the HFE7100 liquid surface, the central jet arising from the surface of sufficiently deep liquid layers after the impact, did not break-up. Therefore, they concluded that the critical Weber number for the central jet break-up of water- HFE7100 impact is not defined.

Cossali et. al [3] studied the time evolution of different parameters such as the crown diameters, height and vertical velocity and mean size of the secondary drops diameters through performing experiments on water droplets impinging onto thin liquid films. The mass and diameter ratios of the secondary drops to the primary drop were investigated experimentally by Okawa et. al [6]. Further studies are those of Rioboo et. al [10], Vander Wal et. al [2] and Pan et. al [11], where droplet impact on liquid film was investigated experimentally.

As a conventional approach to simulate problems involving interfacial dynamics, the Navier-Stokes equations are typically solved using the control volume method along with an interface tracking method such as the Volume of Fluid (VOF) or the level-set method to track the interface.

Rieber and Frohn [4] performed a three dimensional simulation of the water droplet impact onto thin liquid films using the VOF method. Results showed that the time evolution of the crown diameter is almost independent of the Weber number, but the number of secondary drops increased for higher impact Weber numbers. Asadi and Passandideh-Fard [12] performed a 2D axisymmetric simulation utilizing the VOF method and validated the simulation by comparing the time evolution of the nondimensional crown height and diameters with the experimental data in the literature. They also proposed simple correlations for nondimensional parameters involved in the phenomenon. Lee et. al [13] used the level-set method in a 2D axisymmetric coordinates. Guo et. al [14] implemented the combined level set and VOF method (CLSVOF) to investigate the subject in 2D coordinates.

As an alternative approach, the Lattice Boltzmann Method (LBM) has been proved to be a simple but powerful method for simulation of various physical problems, especially multiphase flows where the beauty of the method is more recognized. In contrast to the macroscopic methods, there is no need to track the interface any longer due to the consistent kinetic nature of the LBM and interface formation. Among different multiphase models in the LBM, the Shan and Chen pseudo-potential model [15,16], the free energy model [17], and the model by He et. al [18] are widely used. All these models, however, suffer from different problems including low density ratio limitation. Therefore, many researches have been conducted to overcome the problems of each model, leading to new modified models with considerable success.

The available studies in the literature on the LBM method particularly for investigating droplet impact on liquid films are limited. Lee and Lin [19] in their proposed model for simulating incompressible two phase flows at high density ratios which is based on the He et. al model, simulated a 2D droplet impact on a thin liquid film as a validation of their model. In their study, however, only the effect of the Reynolds number up to 500 was shown and other parameters like the Weber number, the dimensionless film thickness and the density ratio were held constant. Based on the He et. al model, Guo and Wang [20] investigated the effect of density ratio on the splash shape in two dimensional coordinates. Cheng and Lou [21] performed a three dimensional simulation using the free energy model to study the effect of oblique drop impact at a density ratio of 100 and a relatively high Re number of 2000.

Among the two phase models, the pseudo-potential model benefits from the simplicity and computational efficiency. This model, however, has various drawbacks including: the low density ratios limitation; presence of high spurious currents at the interface; coupling between the surface tension and density ratio; thermodynamic inconsistency; and instability at low viscosities. These drawbacks prevent the use of this model in simulating many realistic multiphase problems. Therefore, from the introduction of this model, many studies have been accomplished to overcome or alleviate the above drawbacks. In this paper, the pseudo-potential based model of Li and Luo [1] is implemented to study the effect of the kinematic viscosity ratio of gas to liquid and the density ratio of liquid to gas on a droplet impact onto a thin liquid film. The model has certain capabilities which make it applicable to cases with large density ratios, low viscosities, and tunable values of surface tension independent of the density ratio.

2. NUMERICAL METHOD

The lattice Boltzmann equation with the popular single relaxation time BGK collision operator and a force term is expressed as [22] :

$$f_\alpha(\mathbf{x}+\mathbf{e}_\alpha\delta t,\ t+\delta t)-f_\alpha(\mathbf{x},\ t)= -\frac{1}{\tau}\left(f_\alpha(\mathbf{x},\ t)-f_\alpha^{eq}(\mathbf{x},\ t)\right)+\delta t\mathbf{F}_\alpha \tag{1}$$

where $\mathbf{x}$ is the spatial position, $\mathbf{e}_\alpha$ the discrete velocity in the αth direction, δt the time step, τ the relaxation time, $\mathbf{F}_\alpha$ the forcing term, and f_α and f_α^{eq} represent the particle distribution and the equilibrium distribution functions in the αth direction, respectively. For incompressible flows:

$$f_\alpha^{eq}=\omega_\alpha\rho\left[1+\frac{\mathbf{e}_\alpha\cdot\mathbf{v}}{c_s^2}+\frac{(\mathbf{e}_\alpha\cdot\mathbf{v})^2}{2c_s^4}-\frac{\mathbf{v}\cdot\mathbf{v}}{2c_s^2}\right] \tag{2}$$

where ω_α is the weight factor in the αth direction and c_s is the sound speed in lattice which is equal to $c/\sqrt{3}$ where $c=\delta x/\delta t$. ρ and $\mathbf{v}$ are the macroscopic density and velocity, respectively.

For the D2Q9 lattice used in this paper, the discrete velocities and the weight factors are given by:

$$\mathbf{e}_\alpha=\begin{bmatrix}0&1&0&-1&0&1&-1&-1&1\\0&0&1&0&-1&1&1&-1&-1\end{bmatrix} \tag{3}$$

$$\omega_\alpha=\begin{cases}\frac{4}{9} & \alpha=0\\ \frac{1}{9} & \alpha=1,2,3,4\\ \frac{1}{36} & \alpha=5,6,7,8\end{cases} \tag{4}$$

Guo et al. [22] by considering the effects of the discrete lattice Boltzmann on the forcing term, acquired a forcing scheme which exactly recovers the macroscopic mass conservation equation and the Navier-Stokes equations. However, using this scheme in the Shan and Chen pseudo-potential multiphase model does not work for the relatively large density ratios and is stable only in a very narrow temperature ratio range [23,24]. Li et al. [24] proposed an improved forcing scheme which is stable at higher density ratios by using a modified velocity in the Guo force scheme as follows:

$$\mathbf{F}_\alpha=\omega_\alpha\delta t\left(1-\frac{1}{2\tau}\right)\left[\frac{\mathbf{e}_\alpha-\mathbf{v}'}{c_s^2}+\frac{(\mathbf{e}_\alpha\cdot\mathbf{v}')}{c_s^4}\mathbf{e}_\alpha\right]\cdot\mathbf{F} \tag{5}$$

where $\mathbf{v}'$ is the modified velocity given by the equation $\mathbf{v}'=\mathbf{v}+\epsilon\mathbf{F}/\left((\tau-0.5)\psi^2\right)$ in which ϵ is a constant that can be tuned to achieve thermodynamic consistency (setting ϵ = 0 gives the Guo forcing scheme). ψ is the effective mass which is a function of the local density of the fluid and $\mathbf{F}$ is the summation of all forces exerted on each fluid particle defined in this paper as $\mathbf{F}=\mathbf{F}_1+\mathbf{F}_2$ where $\mathbf{F}_1$ is the fluid-fluid interaction force and $\mathbf{F}_2$ is the fluid-solid interaction force. In this paper concentration is on the early stages of the droplet impact which the effect of gravity is negligible [19].

In order to further improve the stability of the numerical model and, therefore, achieve higher density ratios and lower viscosities, the Multi-Relaxation Time (MRT) collision operator is implemented. The MRT lattice Boltzmann equation for multiphase flows is expressed as follows [25]:

$$f_\alpha(\mathbf{x}+\mathbf{e}_\alpha\delta t,\ t+\delta t)-f_\alpha(\mathbf{x},\ t)\ = -\sum_i\Lambda_{\alpha i}\left(f_i-f_i^{eq}\right)+\delta t\left(s_\alpha-\frac{1}{2}\sum_i\Lambda_{\alpha i}s_i\right) \tag{6}$$

where Λ is the relaxation matrix and s is the forcing term.

Comparing the above equation with Eqs. (1) and (5), the force term s is given by the following equation [26]:

$$S_\alpha=\omega_\alpha\left[\frac{\mathbf{e}_\alpha-\mathbf{v}'}{c_s^2}+\frac{(\mathbf{e}_\alpha\cdot\mathbf{v}')}{c_s^4}\mathbf{e}_\alpha\right]\cdot\mathbf{F} \tag{7}$$

It is more convenient to do the collision step in the momentum space, therefore, the right-hand side of Eq. (6) is transformed into the momentum space by multiplying it with the transformation matrix M as follows [25, 27, 28] :

$$\mathbf{M}\ (\mathrm{RHS})=\mathbf{m}=-\sum_i\hat{\Lambda}_{\alpha i}\left(\hat{f}_i-\hat{f}_i^{eq}\right)+\delta t\sum_i\left(I_{\alpha i}-\frac{1}{2}\hat{\Lambda}_{\alpha i}\right)\hat{s}_i \tag{8}$$

where M is the transformation matrix given by :

$$\mathbf{M}=\begin{bmatrix}1&1&1&1&1&1&1&1&1\\-4&-1&-1&-1&-1&2&2&2&2\\4&-2&-2&-2&-2&1&1&1&1\\0&1&0&-1&0&1&-1&-1&1\\0&-2&0&2&0&1&-1&-1&1\\0&0&1&0&-1&1&1&-1&-1\\0&0&-2&0&2&1&1&-1&-1\\0&1&-1&1&-1&0&0&0&0\\0&0&0&0&0&1&-1&1&-1\end{bmatrix} \tag{9}$$

$$\hat{f}=\mathbf{M}f \tag{10}$$

According to [29]:

$$\hat{f}^{eq}=\mathbf{M}f^{eq}=\rho(1,\ -2+3|\mathbf{v}|^2,\ 1-3|\mathbf{v}|^2,\ v_x,\ -v_x,\ v_y,\ -v_y,\ v_x^2-v_y^2,\ v_xv_y)^T \tag{11}$$

I is the identity matrix and $\hat{\Lambda}$ is the diagonal relaxation matrix in the moment space defined as [29]:

$$\hat{\Lambda} = \mathbf{M}\Lambda\mathbf{M}^{-1} = diag(s_1, s_2, s_3, s_4, s_5, s_6, s_7, s_8, s_9) \\ = diag(\tau_\rho^{-1}, \tau_e^{-1}, \tau_\varsigma^{-1}, \tau_j^{-1}, \tau_q^{-1}, \tau_j^{-1}, \tau_q^{-1}, \tau_\upsilon^{-1}, \tau_\upsilon^{-1}) \quad (12)$$

where ρ is the density, e stands for the energy, and ζ is related to the energy square. j is the momentum, q the energy flux, and υ is the kinematic viscosity. It is worth mentioning that since the relaxation matrix is now diagonal in the momentum space, the relaxations of various physical terms are decoupled [27]. The s_1, s_4 and s_6 entities of the relaxation matrix must be equal to each other and are taken to be one. Thus, s_2, s_3, $s_5 = s_7$ and $s_8 = s_9$ can be tuned separately to achieve higher stability. s_2 and $s_8 = s_9$ are related to the bulk viscosity and kinematic viscosity, respectively :

$$\lambda = \left(\frac{1}{s_2} - 0.5\right)c_s^2 \quad (13) \qquad \upsilon = (\tau_\upsilon - 0.5)c_s^2 \quad (14)$$

It has been proved that the viscous relaxation time is a function of the local density which is given by the following linear interpolation [28]:

$$\tau_\upsilon = \tau_g + \frac{\rho - \rho_g}{\rho_l - \rho_g}(\tau_l - \tau_g) \quad (15)$$

where τ_g, τ_l, ρ_g, ρ_l and ρ are the relaxation time for the gas phase, liquid phase, gas and liquid densities, and the local density in the computational domain, respectively. Equation (15) provides tunable kinematic and, as a result, tunable dynamic viscosity ratios. This is because according to Eq. (14), substituting the relaxation time of each phase gives the corresponding kinematic viscosity.

The macroscopic density and velocity are given by:

$$\rho = \sum_\alpha f_\alpha \quad , \quad \rho\mathbf{v} = \sum_\alpha f_\alpha e_\alpha + \frac{\delta t}{2}\mathbf{F} \quad (16)$$

Li. et al [29] proposed the following relation for the force term in the momentum space:

$$\hat{S} = \begin{bmatrix} 0 \\ 6(v_x F_x + v_y F_y) + \frac{12\epsilon|\mathbf{F}|^2}{\psi^2(\frac{1}{s_2} - 0.5)} \\ -6(v_x F_x + v_y F_y) - \frac{12\epsilon|\mathbf{F}|^2}{\psi^2(\frac{1}{s_3} - 0.5)} \\ F_x \\ -F_x \\ F_y \\ -F_y \\ 2(v_x F_x - v_y F_y) \\ v_x F_y + v_y F_x \end{bmatrix} \quad (17)$$

In order to tune the surface tension independent of the density ratio, Li et al. [1] added a source term to the MRT LB equation which modifies Eq. (8) as follows:

$$\mathbf{m} = -\sum_i \hat{\Lambda}_{\alpha i}\left(\hat{f}_i - \hat{f}_i^{eq}\right) + \delta t \sum_i \left(I_{\alpha i} - \frac{1}{2}\hat{\Lambda}_{\alpha i}\right)\hat{s}_i + \delta t C_\alpha \quad (18)$$

where the source term C is given by :

$$C = \begin{bmatrix} 0 \\ 1.5\tau_e^{-1}(Q_{xx} + Q_{yy}) \\ -1.5\tau_\zeta^{-1}(Q_{xx} + Q_{yy}) \\ 0 \\ 0 \\ 0 \\ 0 \\ -\tau_\upsilon^{-1}(Q_{xx} - Q_{yy}) \\ -\tau_\upsilon^{-1}Q_{xy} \end{bmatrix} \quad (19)$$

where Q_{xx}, Q_{xy} , and Q_{yy} are obtained using the equation:

$$Q = \kappa\frac{G}{2}\psi(\mathbf{x},t)\left[\sum_\alpha w\left(|\mathbf{e}_\alpha|^2\right)\left[\psi(\mathbf{x}+\mathbf{e}_\alpha, t) - \psi(\mathbf{x},t)\right]\mathbf{e}_\alpha\mathbf{e}_\alpha\right] \quad (20)$$

where κ is a coefficient which tunes the surface tension. G = -1 and $w(1) = 1/3$, $w(2) = 1/12$ are the weights in the D2Q9 lattice model. The streaming step is still performed in the velocity space and, therefore, the collision term (Eq. 18) is transformed back into the velocity space, therefore, the streaming step is:

$$f_\alpha(\mathbf{x} + \mathbf{e}_\alpha\delta t,\ t + \delta t) - f_\alpha(\mathbf{x},\ t) = \mathbf{M}^{-1}\mathbf{m} \quad (21)$$

The fluid-fluid interaction force is given by:

$$\mathbf{F}_1(\mathbf{x},t) = -G\psi(\mathbf{x},t)\left[\sum_\alpha w\left(|\mathbf{e}_\alpha|^2\right)\psi(\mathbf{x}+\mathbf{e}_\alpha, t)\mathbf{e}_\alpha\right] \quad (22)$$

$$\psi = \sqrt{\frac{2\left(P_{EOS} - \rho c_s^2\right)}{Gc^2}} \quad (23)$$

where c = 1. The Carnahan-Starling equation of state (EOS) is used in this paper :

$$P_{EOS} = \rho RT\,\frac{1 + b\rho/4 + (b\rho/4)^2 - (b\rho/4)^3}{(1 - b\rho/4)^3} - a\rho^2 \quad (24)$$

The critical temperature is $T_c = 0.3773a/(bR)$, b = 4, R = 1. The parameter a affects the interface thickness; reducing its value gives thicker interface which leads to smaller spurious currents and higher stability, especially at high density ratios. Therefore, in this paper a is set to be 0.25 at high density ratios.

The fluid-solid interaction force is similarly given by:

$$\mathbf{F}_2(\mathbf{x},t) = -G\psi(\mathbf{x},t)\left[\sum_{\alpha} w\left(|\mathbf{e}_\alpha|^2\right)\psi(\rho_w)S(\mathbf{x}+\mathbf{e}_\alpha)\mathbf{e}_\alpha\right] \quad (25)$$

where ρ_w is a fictitious wall density varied to achieve different contact angles. S is equal to one for solid nodes and zero elsewhere.

3. MODEL VALIDATION

In order to validate the developed LBM model, two cases are considered. In the first case, the coexistence values from the numerical model are compared to those of the analytical solution of the Maxwell construction. A liquid film with thickness of 50 lattice units is placed at the center of a 200 ×200 lattice domain using the following relation:

$$\rho = \rho_g + \frac{\rho_l - \rho_g}{2}\left[\tanh(y_1) - \tanh(y_2)\right] \quad (26)$$

where y_1 = 2(y-75)/5 and y_2 = 2(y-125)/5. The liquid film is then let to be equilibrated for 10,000 time steps. The periodic boundary condition is applied in all sides of the domain. The relaxation times for both phases is set to be τ_v = 0.6, $s_2 = s_3$ = 0.51, $s_5 = s_7$ = 1.1 and ϵ is set to be 0.114. The parameter a in the EOS (Eq. 24) is set to be 0.25 for temperature ratios less than 0.6 and 0.5 for others. Figure 1 compares the variation of T/T_c vs. density obtained from the analytical solution of the Maxwell construction and that of the simulation where an excellent agreement between the two results is observed.

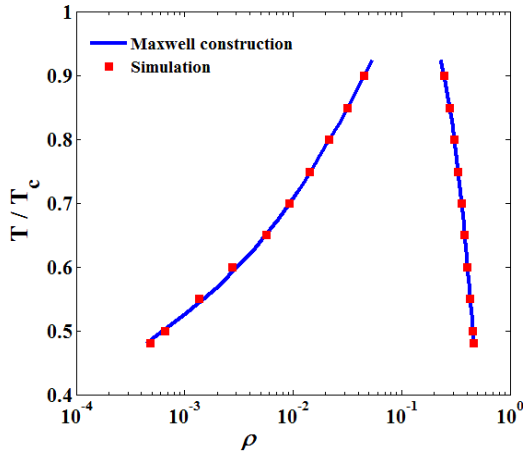

Fig. 1: Comparison of numerical coexistence values with those of Maxwell construction.

Some of the coexistence values are shown in Table 1 for completeness. It was found that τ_v value does not change the coexistence values considerably.

The second case considered is the evaluation of the Laplace law, $\Delta P = \sigma/R_0$ in which σ is the surface tension and R_o is the drop radius. The Laplace law

	ρ_l/ρ_g	
T/T_c	**Numerical**	**Maxwell construction**
0.7	0.358 / 0.00921	0.358 / 0.0093
0.6	0.406 / 0.00273	0.406 / 0.003
0.48	0.464 / 0.000483	0.464 / 0.000445

Table 1: Some coexistence values obtained from numerical model compared with those of the Maxwell construction.

states that the pressure difference between the inside and outside of the droplet is linearly related to the inverse of the droplet radius with the surface tension as the proportionality factor. A droplet is placed at the center of the domain by using the following equation defining the initial density distribution:

$$\rho = \frac{\rho_l + \rho_g}{2} - \frac{\rho_l - \rho_g}{2}\tanh\left[\frac{2\left(\sqrt{(x-x_0)^2 + (y-y_0)^2} - R_0\right)}{5}\right] \quad (27)$$

where x_0 and y_0 are the domain center coordinates which here are equal to 100. Other input parameters (τ_v, s_2=s_3, s_5=s_7, ϵ, and a) are kept the same as in the previous case. Figure 2 shows the results of the simulation at T/T_c = 0.48.

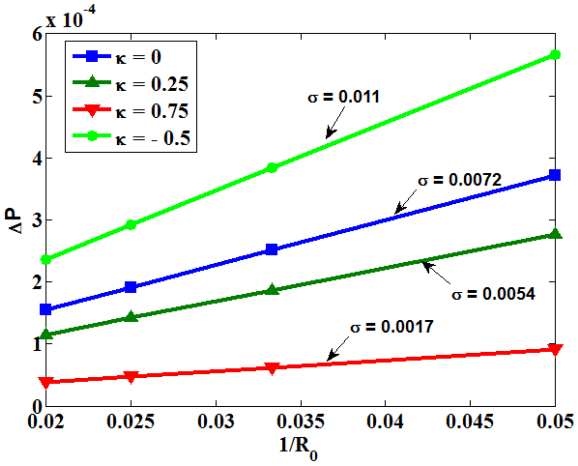

Fig. 2: Evaluation of Laplace law at T/T_c = 0.48.

As it can be seen from the figure, there is a linear relationship between the pressure difference and inverse of the droplet radius for different values of κ. Therefore, the model results agree with those of the Laplace law and at the same time tunable surface tension values independent of the density ratio are possible in the numerical model.

4. RESULTS AND DISCUSSION

Figure 3 shows the time evolution of the droplet impact onto a thin liquid film with a dimensionless time ($t^* = tV/D$) interval of 0.3. V is the droplet impact velocity equal to 0.12, D = 80 is its diameter, and t the time in lattice units. The density ratio is approximately 1000 corresponding to temperature ratio of 0.48. Dimensionless film thickness ($H^*=H/D$) is 0.25. H is being the liquid film thickness equal to 20. The liquid kinematic viscosity $\nu_l = 0.0067$ which gives $Re = VD/\upsilon_l = 1440$. κ is set to be 0.6 which leads to σ = 0.003 and $We = \rho_l V^2 D/\sigma = 178$. The Ohnesorge number, $Oh = \sqrt{We}/Re = \mu_l / (\rho_l \sigma D)^{1/2}$ equals to 0.0093 and the kinematic viscosity ratio of gas to liquid is 5 which is the result of setting the viscous relaxation time $\tau_g = 0.6$ and $\tau_l = 0.52$. The other relaxation times and ϵ are the same as those mentioned in previous cases in Section 3. The bounce back no slip boundary condition is imposed at top and bottom and the periodic boundary condition at two sides of a 400×300 domain. The droplet is assumed to touch the liquid film at time equal zero (t=0). As the figure shows, the droplet spreads radially outward on the liquid film pushing the liquid up to the formation of a crown which is widening with time. The tip of the crown after a certain time is seen to break up forming secondary droplets at the rim.

The effect of the viscosity ratio on the splashing of droplet impact onto the liquid film is displayed in Fig. 4. The kinematic (and as a result, the dynamic) viscosity ratio is changed through varying the gas viscosity while the liquid viscosity is kept constant; this means that the Reynolds number remains unchanged for various kinematic viscosity ratios. The figure shows that the viscosity ratio plays an important role in the splashing phenomenon. When the kinematic viscosity ratio of the gas to liquid is high (above 150), no secondary droplets are generated (see Fig. 4c). As the gas viscosity is decreased, however, the splashing leads to liquid breakup and separation of the secondary droplets. The number of these secondary droplets increases by further reduction of the viscosity ratio as depicted in Fig. 4a.

To evaluate the effect of the liquid to gas density ratio on droplet impact, a low ratio of 10 is selected to be compared with the results of a high density ratio of 1000. The kinematic viscosity ratio and the dimensionless film thickness are the same as the values related to Fig. 3. The Reynolds and Weber numbers are 1520 and 200, respectively, which are close to the simulation values for a density ratio of 1000. Figure 5 shows the time evolution of impact dynamics with a time interval of 0.325 indicating that the density ratio has a significant effect on the impact phenomenon. Since the gas density is considerable at the density ratio of 10, it prevents the liquid rise from the surface to move freely in both radial and vertical directions leading to the formation of an inward liquid turn on top of the raised liquid sheet.

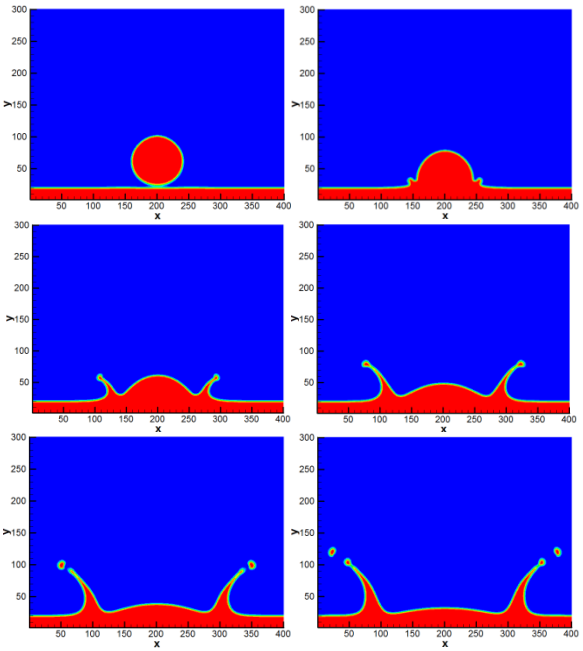

Fig. 3: Time evolution of a droplet impact onto a thin liquid film. $\rho_l/\rho_g = 1000, \upsilon_g/\upsilon_l = 5$, H* = 0.25, Re = 1440, We = 178, and Oh=0.0093. Time interval = 0.3

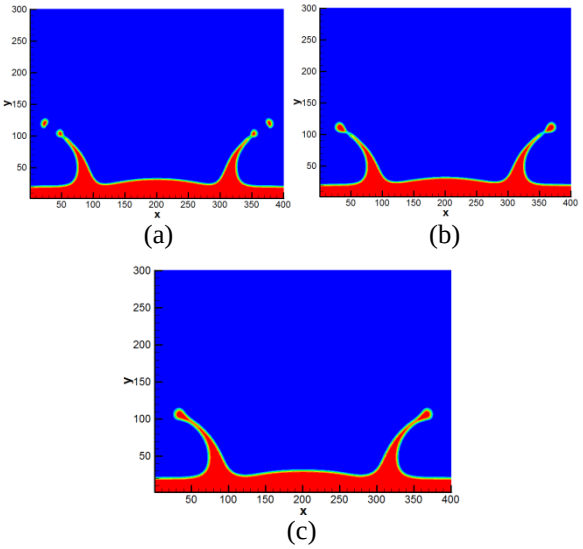

(a) (b) (c)

Fig. 4: The effect of viscosity ratio on the impact for a gas to liquid kinematic viscosity ratio of (a): 5, (b): 50, (c): 150. $\rho_l/\rho_g = 1000$, H*=0.25, Re = 1440, We = 178, and Oh=0.0093. The images belong to t*= 1.5.

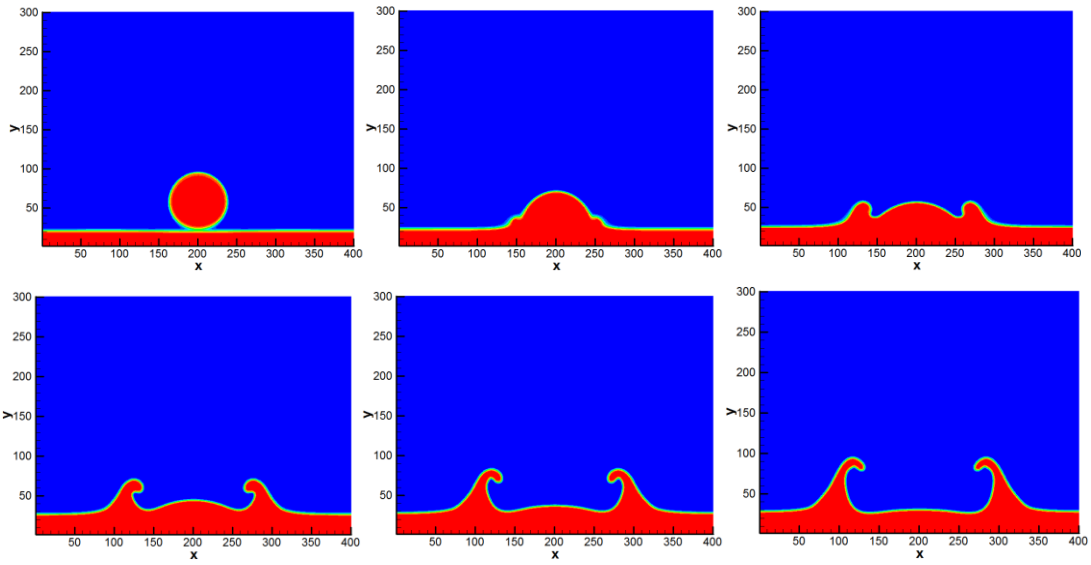

Fig. 5: Time evolution of a droplet impact onto a thin liquid film. $\rho_l/\rho_g = 10, \upsilon_g/\upsilon_l = 5$, H* = 0.25, Re = 1520 and We = 200. The time interval between images is 0.325.

5. CONCLUSION

In this paper a MRT lattice Boltzmann model was implemented to study the droplet impact on a thin liquid film. The multiphase model is based on the pseudo-potential multiphase model.

According to the simulation results of the developed numerical model in this paper, the following conclusions are made:

- Simulation results can be obtained at density ratios as high as 1000.
- The coexistence values agree well with those of the analytical solutions at a wide range of the temperature ratio.
- Surface tension in the model can be varied independent of the density ratio.
- The LBM model can predict the underlying physics of droplet impact such as crown formation, and separation of secondary droplets from top of the crown.
- Viscosity ratio plays an important role on size and number of secondary droplets separated from the crown. A higher kinematic viscosity ratio of gas to liquid results in a smaller number of secondary droplets with larger size.
- The shape of the liquid rise from the liquid film at low density ratios like 10 is completely different with the crown shape observed at density ratio of 1000.

REFERENCES

[1] Q. Li and K. Luo. Achieving tunable surface tension in the pseudopotential lattice Boltzmann modeling of multiphase flows. *Physical Review E*, 88(5):053307, 2013

[2] R.L. Vander Wal, G.M. Berger and S.D. Mozes. Droplets splashing upon films of the same fluid of various depths. *Experiments in fluids*, 40(1):33-52, 2006

[3] G. Cossali, M. Marengo, A. Coghe and S. Zhdanov. The role of time in single drop splash on thin film. *Experiments in Fluids*, 36(6):888-900, 2004

[4] M. Rieber and A. Frohn. A numerical study on the mechanism of splashing. *International Journal of Heat and Fluid Flow*, 20(5):455-461, 1999

[5] M. Rein. Phenomena of liquid drop impact on solid and liquid surfaces. *Fluid Dynamics Research*, 12(2):61-93, 1993

[6] T. Okawa, T. Shiraishi and T. Mori. Production of secondary drops during the single water drop impact onto a plane water surface. *Experiments in fluids*, 41(6):965-974, 2006

[7] A. Yarin and D. Weiss. Impact of drops on solid surfaces: self-similar capillary waves, and splashing as a new type of kinematic discontinuity. *Journal of Fluid Mechanics*, 283:141-173, 1995

[8] A.-B. Wang and C.-C. Chen. Splashing impact of a single drop onto very thin liquid films.

Physics of Fluids (1994-present), 12(9):2155-2158, 2000

[9] S. Manzello and J. Yang. An experimental study of a water droplet impinging on a liquid surface. *Experiments in fluids*, 32(5):580-589, 2002

[10] R. Rioboo, C. Bauthier, J. Conti, M. Voue´and J. De Coninck. Experimental investigation of splash and crown formation during single drop impact on wetted surfaces. *Experiments in fluids*, 35(6):648-652, 2003

[11] K.-L. Pan, K.-R. Cheng, P.-C. Chou and C.-H. Wang. Collision dynamics of high-speed droplets upon layers of variable thickness. *Experiments in Fluids*, 45(3):435-446, 2008

[12] S. Asadi and M. Passandideh Fard. A computational study of droplet impingement onto a thin liquid film. *Arabian Journal for Science and Engineering*, 34:505-517, 2009

[13] S.H. Lee, N. Hur and S. Kang. A numerical analysis of drop impact on liquid film by using a level set method. *Journal of mechanical science and technology*, 25(10):2567-2572, 2011

[14] Y. Guo, L.Wei, G. Liang and S. Shen. Simulation of droplet impact on liquid film with CLSVOF. *International Communications in Heat and Mass Transfer*, 53:26-33, 2014

[15] X. Shan and H. Chen. Lattice Boltzmann model for simulating flows with multiple phases and components. *Physical Review E*, 47(3):1815, 1993

[16] X. Shan and H. Chen. Simulation of nonideal gases and liquid-gas phase transitions by the lattice Boltzmann equation. *Physical Review E*, 49(4):2941, 1994

[17] M.R. Swift, E. Orlandini, W.R. Osborn and J. M. Yeomans. Lattice Boltzmann simulations of liquid-gas and binary fluid systems. *Physical Review E*, 54(5):5041, 1996

[18] X. He, S. Chen and R. Zhang. A lattice Boltzmann scheme for incompressible multiphase flow and its application in simulation of Rayleigh–Taylor instability. *Journal of Computational Physics*, 152(2):642-663, 1999

[19] T. Lee and C.-L. Lin. A stable discretization of the lattice Boltzmann equation for simulation of incompressible two-phase flows at high density ratio. *Journal of Computational Physics*, 206(1):16-47, 2005

[20] J.-h. GUO and X.-y. WANG. Simulation of the two phase flow of droplet impingement on liquid film by the lattice boltzmann method. *Journal of Hydrodynamics, Ser. B*, 24(2):292-297, 2012

[21] M. Cheng and J. Lou. A numerical study on splash of oblique drop impact on wet walls. *Computers & Fluids*, 115:11-24, 2015

[22] Z. Guo, C. Zheng and B. Shi. Discrete lattice effects on the forcing term in the lattice Boltzmann method. *Physical Review E*, 65(4):046308, 2002

[23] L. Chen, Q. Kang, Y. Mu, Y.-L. He and W.-Q. Tao. A critical review of the pseudopotential multiphase lattice Boltzmann model: Methods and applications. *International Journal of Heat and Mass Transfer*, 76:210-236, 2014

[24] Q. Li, K. Luo and X. Li. Forcing scheme in pseudopotential lattice Boltzmann model for multiphase flows. *Physical Review E*, 86(1):016709, 2012

[25] M.E. McCracken and J. Abraham. Multiple-relaxation-time lattice-Boltzmann model for multiphase flow. *Physical Review E*, 71(3):036701, 2005

[26] D. Zhang, K. Papadikis and S. Gu. Three-dimensional multi-relaxation time lattice-Boltzmann model for the drop impact on a dry surface at large density ratio. *International Journal of Multiphase Flow*, 64:11-18, 2014

[27] Z. Yu and L.-S. Fan. Multirelaxation-time interaction-potential-based lattice Boltzmann model for two-phase flow. *Physical Review E*, 82(4):046708, 2010

[28] S. Mukherjee and J. Abraham. A pressure-evolution-based multi-relaxation-time high-density-ratio two-phase lattice-Boltzmann model. *Computers & fluids*, 36(6):1149-1158, 2007

[29] Q. Li, K. Luo and X. Li. Lattice Boltzmann modeling of multiphase flows at large density ratio with an improved pseudopotential model. *Physical Review E*, 87(5):053301, 2013